it is doubtful that the central acetate is uncoordinated for any significant period of time. In our work, partial deuteriation allowed the assignment of the central acetate resonances. While the two resonances stemming from this group were quite close in chemical shift for the Pr(III) complex, they differ by 24 ppm in the Yb(III) complex.

These results are consistent with the solid-state structures of both Nd- and Gd(DTPA)$^{2-}$ as well as certain solution-state properties. From a correlation of luminescence wavelengths with total charge donated from a given ligand, Albin and Horrocks estimated the charge on Eu(DTPA)$^{2-}$ to be −5.3, implying full coordination by all five acetates.[31] Additionally, water $^1$H relaxation data for Gd(DTPA)$^{2-}$[32] and luminescence studies on the Eu(III) complex[33] are consistent with a single coordinated water molecule as found in the crystal structures mentioned above; this supports the coordination of the central acetate since its displacement should open up an additional coordination site for water.

## Conclusions

In conclusion, we have demonstrated that 2D NMR methods can play a vital role in assignment of the solution structural properties of lanthanide chelates. In solution, Ln(DTPA)$^{2-}$ chelates undergo a dynamic exchange between two enantiomers. This isomerization involves exchanges of coordinated terminal acetates between the top and bottom faces of the square-antiprismatic complex. The rates of this exchange process are similar to those seen in the macrocyclic chelates Ln(DOTA)$^-$ and Ln(TETA)$^-$. Calculation of the chemical shifts for the Ln(DTPA)$^{2-}$ chelate protons reveals that the shifts are predominantly dipolar in origin. These calculations clearly demonstrate that assignment of resonances (and hence geometry) merely by obtaining good fits between observed and calculated numbers is quite dangerous. The use of COSY and EXSY data provides invaluable evidence that can be used to constrain the fits and provide clear-cut answers to which fits among the number of possible fits are wrong. The solution structure of the chelates (including coordination of the central acetate) agrees well with the crystal structures determined for Gd(DTPA)$^{2-}$ and Nd(DTPA)$^{2-}$.

**Acknowledgment.** This work was supported by PHS Grant GM37777, awarded by the National Institute of General Medical Sciences. NMR experiments at 500 MHz were run at the Francis Bitter National Magnet Laboratory, MIT, supported by Grant RR00995 from the Division of Research Resources of the NIH and Contract C-670 from the National Science Foundation. We thank Dr. A. Dean Sherry for providing a copy of his computer program for performing chemical shift calculations.

**Registry No.** [Pr(DTPA)(H$_2$O)]$^{2-}$, 76147-47-2; [Eu(DTPA)(H$_2$O)]$^{2-}$, 76166-31-9; [Yb(DTPA)(H$_2$O)]$^{2-}$, 76147-40-5.

---

(31) Albin, M.; Horrocks, W. D. *Inorg. Chem.* **1985**, *24*, 895.

(32) Koenig, S. H.; Brown, R. D., III. In *Magnetic Resonance Annual*; Kressel, H. Y., Ed.; Raven Press: New York, 1987.

(33) Bryden, C. C.; Reilley, C. N. *Anal. Chem.* **1982**, *54*, 610.

---

Contribution from the Department of Chemistry, Emory University, Atlanta, Georgia 30322, and Dipartimento di Scienze Chimiche, Università di Trieste, 34127 Trieste, Italy

# Organocobalt B$_{12}$ Models Bearing Axial Substituents on a Costa-Type Equatorial Ligand: Structural, Rate, and Spectroscopic Consequences

Paulos G. Yohannes,[†] Nevenka Bresciani-Pahor,[‡] Lucio Randaccio,*[,‡] Ennio Zangrando,[‡]
and Luigi G. Marzilli*[,†]

*Received March 25, 1988*

Several new organocobalt complexes of the type [LCo((DO)(DOH)Me$_2$pn)CH$_3$]X were synthesized from Co((DO)(DOH)Me$_2$pn)Br$_2$, where L = neutral N- or P-donor ligand and (DO)(DOH)Me$_2$pn = $N^2,N^{2'}$-2,2-dimethylpropanediylbis(2,3-butanedione 2-imine 3-oxime). These were characterized by $^1$H NMR spectroscopy and, in a few cases, by $^{13}$C NMR spectroscopy. The rates of L ligand dissociation were found to be greater than those of the analogous Costa model complexes, where the equatorial ligand, (DO)(DOH)pn, has a propylene bridge in place of the 2,2-dimethylpropylene bridge, or the analogous cobaloxime complexes. The three-dimensional structures of two of these new complexes, [LCo((DO)(DOH)Me$_2$pn)CH$_3$]PF$_6$, in which L = pyridine (py) (I) and L = 1,5,6-trimethylbenzimidazole (Me$_3$Bzm) (II), were determined. Crystallographic details are as follows: I, $C_{19}H_{31}CoF_6N_5O_2P$, $P2_12_12_1$, $a$ = 12.718 (3) Å, $b$ = 12.861 (2) Å, $c$ = 15.437 (3) Å, $D$(calcd) = 1.49 g cm$^{-3}$, $Z$ = 4, $R$ = 0.048 for 2923 independent reflections; II, $C_{24}H_{38}CoF_6N_6O_2P\cdot{}^1/_2H_2O$, *Pbca*, $a$ = 14.103 (3) Å, $b$ = 17.415 (2) Å, $c$ = 24.555 (3) Å, $D$(calcd) = 1.44 g cm$^{-3}$, $Z$ = 8, $R$ = 0.048 for 3208 independent reflections. The structures of these two derivatives are similar to those of the analogous (DO)(DOH)pn compounds, except that the planar py and Me$_3$Bzm ligands lean away from the 2,2-dimethylpropylene group. The plane of L makes an angle of ~80° with the plane of the equatorial ligand. This result is attributed to steric effects. These steric effects are believed to account for the increased rate of L dissociation compared to that in the parent model system. In addition, $^1$H and $^{13}$C chemical shifts of L are upfield in the (DO)(DOH)Me$_2$pn componds. This observation is attributed to equatorial ligand anisotropy and strongly indicates that $^1$H and $^{13}$C NMR shifts of L in organocobalt models reflect ligand anisotropy, as well as Co anisotropy.

## Introduction

With the growing recognition that the role of the Co center in coenzyme B$_{12}$ (5′-deoxyadenosylcobalamin) dependent enzymic processes is probably limited to providing a facile source of 5′-deoxyadenosyl radical via Co–C bond homolysis,[1,2] interest has refocused on the factors promoting cleavage of this bond.[1-4] Conformational changes in the coenzyme that accompany substrate-induced conformational changes in the B$_{12}$ holoenzymes are almost certainly responsible for promoting cleavage.[1-4] For some time, we have been interested in elucidating changes in conformation of organocobalt species that promote cleavage.[3-5]

---

[†] Emory University.

[‡] Università di Trieste.

(1) Halpern, J. *Science* (*Washington, D.C.*) **1985**, *227*, 869. Halpern, J.; Kim, S. H.; Leung, T. W. *J. Am. Chem. Soc.* **1984**, *106*, 8317. Halpern, J. *Pure Appl. Chem.* **1983**, *55*, 1059. Halpern, J. In *B$_{12}$*; Dolphin, D., Ed.; Wiley: New York, 1982; Vol. 1, p 501. Ng, F. T.; Rempel, G. L.; Halpern, J. *Inorg. Chim. Acta* **1983**, *77*, L65. Halpern, J. *Ann. N.Y. Acad. Sci.* (*U.S.A.*) **1974**, *239*, 2.

(2) Finke, R. J.; Schiraldi, D. A.; Mayer, B. J. *Coord. Chem. Rev.* **1984**, *31*, 105. Finke, R. G.; Hay, B. P. *Inorg. Chem.* **1984**, *23*, 3041. Hay, B. P.; Finke, R. J. *J. Am. Chem. Soc.* **1986**, *108*, 4820. Hay, B. P.; Finke, R. G. *J. Am. Chem. Soc.* **1987**, *109*, 8012.

(3) Bresciani-Pahor, N.; Forcolin, M.; Marzilli, L. G.; Randaccio, L.; Summers, M. F.; Toscano, P. J. *Coord. Chem. Rev.* **1985**, *63*, 1.

0020-1669/88/1327-4738$01.50/0

In the absence of crystalline holoenzymes, NMR spectroscopy offers the best hope for identifying structural/conformational changes in the holoenzymes.[5] It is now clear that relationships exist between $^1H$, $^{13}C$, and $^{31}P$ NMR chemical shifts and the structure, rate, and equilibrium processes in several series of organocobalt compounds, including cobalamins.[5-10]

Simple model compounds afford well-defined relationships between structure and spectroscopic and other solution properties. However, in cobalamins, the structures are less well defined because of both numerous waters of crystallization and disorder in the acetamide and propionamide side chains that extend above and below the corrin ring.[10-12] In this study, we have examined complexes of a simple equatorial ligand, (DO)(DOH)$Me_2$pn, with methyl substituents on the propylene bridge, viz.

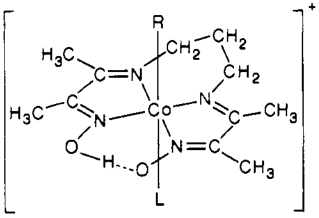

$[LCo((DO)(DOH)pn)R]^+$

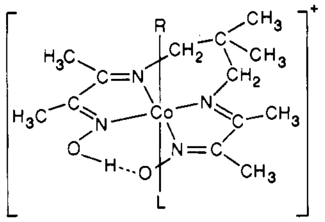

$[LCo((DO)(DOH)Me_2pn)R]^+$

Complexes with the parent (DO)(DOH)pn ligand have received wide attention as a means of assessing fundamental aspects of organocobalt chemistry.[13-15]

These equatorial chelates, CHEL, form Costa-type models, and this is the first report of LCo(CHEL)R complexes with (DO)(DOH)$Me_2$pn, where L = neutral axial ligand and R = alkyl ligand. The most widely studied coenzyme $B_{12}$ models are of the type $LCo(DH)_2R$. In these cobaloximes, DH = monoanion of dimethylglyoxime. Other abbreviations for L are as follows: $Me_3Bzm$, 1,5,6-trimethylbenzimidazole; py, pyridine; 3,5-LUT, 3,5-lutidine; 4-$Me_2$Npy, 4-(dimethylamino)pyridine; 1-MeImd, 1-methylimidazole; 1,2-MeImd, 1,2-dimethylimidazole; $PhNH_2$, aniline; $MeOPhNH_2$, *p*-anisidine; DEA, aminoacetaldehyde dimethyl acetal (2,2-dimethoxyethylamine); $P(OMe)_3$, trimethyl phosphite; $PEtPh_2$, ethyldiphenylphosphine; $POEtPh_2$, ethyl diphenylphosphinite.

## Experimental Section

**Reagents.** $PEtPh_2$ (Strem) and the remaining ligands (Aldrich) were used as received except $P(OMe)_3$, which was distilled. $Me_3Bzm$ was prepared by a standard procedure.[16] Elementary analyses (C, H, N; given in the supplementary material for the organocobalt compounds; Atlantic Microlabs, Atlanta, GA) were satisfactory for all complexes listed in the first column of Table IV.

**Rate Measurements.** Ligand substitution rate studies were performed spectrophotometrically as described previously.[13]

**Data Analysis.** The rate constants are defined as

$$ML \underset{k_{-1}}{\overset{k_1}{\rightleftharpoons}} M + L$$

$$M + L' \xrightarrow{k_2} ML'$$

where M is $Co((DO)(DOH)Me_2pn)CH_3^+$.

**NMR Spectroscopy.** $^1H$ NMR (361.08 MHz) spectra were measured on a Nicolet NB-360 spectrometer and contained 16K data points with a spectral range of 7.2 kHz. All chemical shifts are relative to internal $Me_4Si$ with $CDCl_3$ as solvent unless specified otherwise. $^{13}C$ NMR (75 MHz) spectra were obtained on a General Electric QE-300 spectrometer with a spectral range of 10 kHz. The 1D-NOE experimental procedures were described previously.[9,13] For the 2D-NOE experiments, 512 spectra of 1K data points were collected by using a 90–$\tau$–90–$t_m$–90 acquisition pulse sequence without spinning. The total evolution time ($\tau$) was 330 $\mu$s; the mixing time ($t_m$) was 400 ms. The delay between scans was 1.8 s. Sample concentration was ca. 0.2 M.

**Preparation of $(DOH)_2Me_2pn$.** On the basis of the procedure for making $(DOH)_2$pn,[17] a solution of 2,3-butanedione oxime (119 g, 1.16 mol) and 2,2-dimethyl-1,3-propanediamine (50 g, 0.48 mol) in isopropyl ether (400 mL) was heated at reflux for 7 h. The water (15 mL) produced from the reaction was removed by using a Dean–Stark trap. Solvent was removed on a rotary evaporator until the solution turned cloudy. The mixture was kept at 0 °C overnight to give a white crystalline product, which was collected, washed with petroleum ether, and air-dried: mp 130–133 °C (uncorrected); yield 44 g (34.2%). $^1H$ NMR (acetone-$d_6$, ppm): s, 10.52 (2 H); s, 3.32 (4 H); s, 2.03 (6 H); s, 1.98 (6 H); s, 1.05 (6 H). Anal. Calcd for $C_{13}H_{24}N_4O_2$: C, 58.40; H, 9.01; N, 20.96. Found: C, 58.21; H, 9.11; N, 20.81.

**Preparation of $Co((DO)(DOH)Me_2pn)Br_2$.** A procedure[13] used for making $Co((DO)(DOH)pn)Br_2$ was employed. The ligand, $(DOH)_2Me_2Pn$ (5.5 g, 0.02 mol), was dissolved in acetone (65 mL) and treated with an aqueous solution (30 mL) of $CoBr_2 \cdot xH_2O$ (7.4 g of material stated to contain 40.5% $H_2O$, from Strem Chemicals) and KBr (2.8 g, 0.024 mol). The resulting mixture was stirred vigorously to give a clear solution that was then aerated for 3 h. Acetone was added to replace that lost, and a green solid began to form almost immediately. It was collected, washed with water (300 mL), 95% ethanol (50 mL), and diethyl ether, and air-dried; yield 3.93 g (46%). $^1H$ NMR ($CDCl_3$, ppm): s, 19.12 (1 H); s, 3.90 (4 H); s, 2.65 and s, 2.62 (12 H); s, 1.40 (6 H). Anal. Calcd for $CoC_{13}H_{23}N_4O_2Br_2 \cdot {}^1/_2H_2O$: C, 31.54; H, 4.89; N, 11.32. Found: C, 31.67; H, 4.86; N, 11.36.

**Preparation of $[LCo((DO)(DOH)Me_2pn)CH_3]PF_6$ Complexes.** To avoid cleavage of the Co–C bond, all compounds were handled in low light and at <35 °C.

**$[1\text{-MeImdCo}((DO)(DOH)Me_2pn)CH_3]PF_6$.** A suspension of $Co((DO)(DOH)Me_2pn)Br_2 \cdot {}^1/_2H_2O$ (4.0 g, 8 mmol) in methanol (150 mL) was dissolved by adding three pellets of NaOH (ca. 0.40 g) and 1-MeImd (0.8 mL, 10 mmol). The mixture was stirred vigorously until a clear red solution was obtained. The pH of the solution was adjusted to 7 by adding $HNO_3$ (5 M). The solution was deaerated with prepurified $N_2$ for 10 min. Methyl iodide (1.2 equiv) was added, followed immediately by addition of a solution of $NaBH_4$ (0.44 g, 11.6 mmol) in water (15 mL). The solution was stirred magnetically for an additional 6 min, with $N_2$ passing over the solution. Acetone was then added to quench the reaction, the mixture filtered, and the solvent removed on a rotary evaporator (30 °C). Acetone (100 mL) was added to precipitate any excess salt. The mixture was filtered, the solvent was removed again, and methanol (25 mL) was added to redissolve the product. A methanol solution (15 mL) of $NH_4PF_6$ (3.6 g, 22.1 mmol) was added, and the solution was left in the hood uncovered for 4 h, after which a yellow

---

(4) Marzilli, L. G.; Summers, M. F.; Bresciani-Pahor, N.; Zangrando, E.; Charland, J.-P.; Randaccio, L. *J. Am. Chem. Soc.* **1985**, *107*, 6880. Summers, M. F.; Marzilli, L. G.; Bresciani-Pahor, N.; Randaccio, L. *J. Am. Chem. Soc.* **1984**, *106*, 4478.

(5) Summers, M. F.; Marzilli, L. G.; Bax, A. *J. Am. Chem. Soc.* **1986**, *108*, 4285. Bax, A.; Marzilli, L. G.; Summers, M. F. *J. Am. Chem. Soc.* **1987**, *109*, 566.

(6) Charland, J. P.; Zangrando, E.; Bresciani-Pahor, N.; Randaccio, L.; Marzilli, L. G. Submitted for publication.

(7) Marzilli, L. G.; Bayo, F.; Summers, M. F.; Thomas, L. B.; Zangrando, E.; Bresciani-Pahor, N.; Mari, M.; Randaccio. L. *J. Am. Chem. Soc.* **1987**, *109*, 6045.

(8) Brown, K. L.; Hakimi, J. M. *J. Am. Chem. Soc.* **1986**, *108*, 496. Brown, K. L.; Hakimi, J. M.; Jacobson, D. W. *J. Am. Chem. Soc.* **1984**, *106*, 7894. Brown, K. L. *J. Am. Chem. Soc.* **1987**, *109*, 2277.

(9) Parker, W. O., Jr.; Zangrando, E.; Bresciani-Pahor, N.; Marzilli, P. A.; Randaccio, L.; Marzilli, L. G. *Inorg. Chem.* **1988**, *27*, 2170.

(10) Rossi, M.; Glusker, J. P.; Randaccio, L.; Summers, M. F.; Toscano, P. J.; Marzilli, L. G. *J. Am. Chem. Soc.* **1985**, *107*, 1729.

(11) Glusker, J. In *$B_{12}$*; Dolphin, D., Ed.; Wiley-Interscience: New York, 1982; Vol. 1, p 23.

(12) Alcock, N. W.; Dixon, R. M.; Golding, B. T. *J. Chem. Soc., Chem. Commun.* **1985**, 603.

(13) Parker, W. O., Jr.; Bresciani-Pahor, N.; Zangrando, E.; Randaccio, L.; Marzilli, L. G. *Inorg. Chem.* **1985**, *24*, 3908. Marzilli, L. G.; Bresciani-Pahor, N.; Randaccio, L.; Zangrando, E.; Myers, S. A.; Finke, R. G. *Inorg. Chim. Acta* **1985**, *107*, 139. Parker, W. O., Jr.; Bresciani-Pahor, N.; Zangrando, E.; Randaccio, L.; Marzilli, L. G. *Inorg. Chem.* **1986**, *25*, 1303. Parker, W. O., Jr.; Bresciani-Pahor, N.; Zangrando, E.; Randaccio, L.; Marzilli, L. G. *Inorg. Chem.* **1986**, *25*, 3489.

(14) Costa, G. *Pure Appl. Chem.* **1972**, *30*, 335. Pellizer, G.; Tauszik G. R.; Costa, G. *J. Chem. Soc., Dalton Trans.* **1973**, 317. Pellizer, G.; Tauszik, G. R.; Tauzher, G.; Costa, G. *Inorg. Chim. Acta* **1973**, *7*, 60.

(15) Elliot, C. M.; Hershenhart, E.; Finke, R. G.; Smith, B. L. *J. Am. Chem. Soc.* **1981**, *103*, 5558. Finke, R. G.; Smith, B. L.; Droege, M. W.; Elliot, C. M.; Hershenhart, E. *J. Orgnomet. Chem.* **1980**, *202*, C25. Finke, R. G.; Smith, B. L.; Mayer, B. J.; Molinero, A. A. *Inorg. Chem.* **1983**, *22*, 3677.

(16) Simonav, A. M.; Pozhavskii, A. E.; Marianovskii, V. M. *Indian J. Chem.* **1967**, *5*, 81.

(17) Uhlig, E.; Friederich, M. *Z. Anorg. Allg. Chem.* **1966**, *343*, 299.

**Table I.** Crystallographic Data and Details of Refinements for Compounds I and II

| | I | II |
|---|---|---|
| formula | $C_{19}H_{31}CoF_6N_5O_2P$ | $C_{24}H_{38}CoF_6N_6O_2P\cdot 1/2H_2O$ |
| fw | 565.4 | 655.5 |
| cryst syst | orthorhombic | orthorhombic |
| space group | $P2_12_12_1$ | *Pbca* |
| *a*, Å | 12.718 (3) | 14.103 (3) |
| *b*, Å | 12.861 (2) | 17.415 (2) |
| *c*, Å | 15.437 (3) | 24.555 (3) |
| *V*, Å$^3$ | 2524.8 | 6030.5 |
| *D*(measd), g cm$^{-3}$ | 1.50 | 1.46 |
| *D*(calcd), g cm$^{-3}$ | 1.49 | 1.44 |
| *Z* | 4 | 8 |
| $\mu$, cm$^{-1}$ | 8.1 | 6.9 |
| cryst dimens, cm | 0.05 × 0.06 × 0.07 | 0.02 × 0.03 × 0.06 |
| no. of rflns measd | 3433 | 7231 |
| no. of indep rflns with $I \geq 3\sigma(I)$ | 2923 | 3208 |
| *F*(000) | 1168 | 2728 |
| no. of params defined | 319 | 424 |
| max $2\theta$ | 56 | 54 |
| *R* | 0.048 | 0.048 |
| $R_w$ | 0.057 | 0.051 |

powder was collected, washed with water, and air-dried. Precipitation of the product may be facilitated by adding a small amount of water; yield 1.5 g (31%).

**[Me$_3$BzmCo((DO)(DOH)Me$_2$pn)CH$_3$]PF$_6$.** The procedure described above produced X-ray-quality crystals from acetone–MeOH–H$_2$O (5:1:1 v/v) solution in 2 days by slow evaporation (25 °C); yield 50 mg (8%).

**[H$_2$OCo((DO)(DOH)Me$_2$pn)CH$_3$]PF$_6$.** [1-MeImdCo((DO)(DOH)-Me$_2$pn)CH$_3$]PF$_6$·2H$_2$O (1.2 g, 2.0 mmol) in an aqueous methanol (85%) solution (60 mL) was stirred with 2 g of Dowex 50X8-100 ion-exchange resin (strongly acidic cation) at 30 °C for 8–10 h. After filtration, the solvent was removed at 30 °C on a rotary evaporator. The red-brown solid obtained was then dissolved in acetone (10 mL). Petroleum ether was added to cloudiness, and precipitation was induced when the flask was scratched and cooled (0 °C). A red-brown solid was collected, washed with ether, and air-dried; yield 0.80 g (79%).

**[LCo((DO)(DOH)Me$_2$pn)CH$_3$]PF$_6$ (L = PhNH$_2$, MeOPhNH$_2$, py, 1,2-Me$_2$Imd, 4-Me$_2$Npy, P(OMe)$_3$).** A suspension of [H$_2$OCo((DO)-(DOH)Me$_2$pn)CH$_3$]PF$_6$ (200 mg, 0.40 mmol) in CH$_2$Cl$_2$ (20 mL) was treated with ca. 1.5 equiv of L and stirred at room temperature for 2 h. The resulting solution was filtered to remove any undissolved material, and the solvent was removed on a rotary evaporator. The oily product obtained was dissolved in methanol (5 mL), and this solution was then poured into ice-cold H$_2$O (ca. 50 mL). The solid product formed when this solution was stored at 5 °C was collected after ca. 1 h, washed with water, and air-dried for several hours in the dark. Yields: L = PhNH$_2$, 120 mg (52%); L = MeOPhNH$_2$, 130 mg (52%); L = py, 130 mg (57%); L = 1,2-Me$_2$Imd, 120 mg (51%); L = 4-Me$_2$Npy, 75 mg (31%); L = P(OMe)$_3$, 110 mg (44%). X-ray-quality crystals with L = py were obtained from an aqueous methanol (80%) solution after 2 days at 25 °C.

**[LCo((DO)(DOH)Me$_2$pn)CH$_3$]PF$_6$ (L = PEtPh$_2$, POEtPh$_2$, DEA).** The procedure just described was employed except that diethyl ether instead of water was used to precipitate the products. The yellow products were collected, washed with ether, and air-dried. Yields: L = PEtPh$_2$, 120 mg (43%); L = POEtPh$_2$, 70 mg (24%); L = DEA, 70 mg (30%).

**[(3,5-LUT)Co((DO)(DOH)Me$_2$pn)CH$_3$]PF$_6$.** A CH$_2$Cl$_2$ solution of [H$_2$OCo((DO)(DOH)Me$_2$pn)CH$_3$]PF$_6$ (200 mg, 0.4 mmol) and 3,5-LUT (ca. 1.5 equiv) was stirred for 1 h at room temperature. Petroleum ether was added to cloudiness. The red-brown crystalline product formed after 8 h at 0 °C was collected and washed with petroleum ether; yield 100 mg (42%).

**Crystal Data.** Crystals of [LCo((DO)(DOH)Me$_2$pn)CH$_3$]PF$_6$, where L = py (I) and L = Me$_3$Bzm (II), were obtained as described above. Cell dimensions, determined preliminarily from Weissenberg and precession photographs, were refined from 25 reflections lying in the Θ range 12–17° on an Enraf-Nonius CAD4 single-crystal diffractometer by the $\omega$–$2\theta$ scan technique, using graphite-monochromated Mo K$\alpha$ radiation. The crystal data of interest are given in Table I. Intensities of three standard reflections were measured during the data collection and did not show any systematic decay throughout the data recording. Intensities having $I > 3\sigma(I)$ were corrected for Lorentz and polarization factors and anomalous dispersion. No correction for absorption was included because of the small size of the crystals used and the small values of the absorption coefficients.

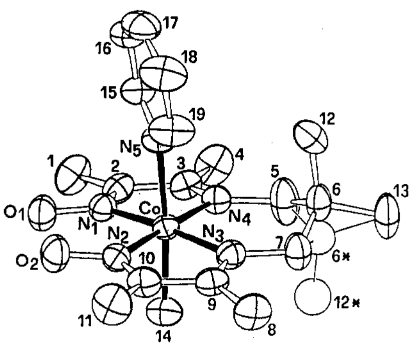

**Figure 1.** ORTEP drawing (50% probability thermal ellipsoids) and labeling scheme for the non-hydrogen atoms of I. Carbon atoms are labeled only by their ordering number in the coordinate list. For the disordered C6* and C12* atoms, see text.

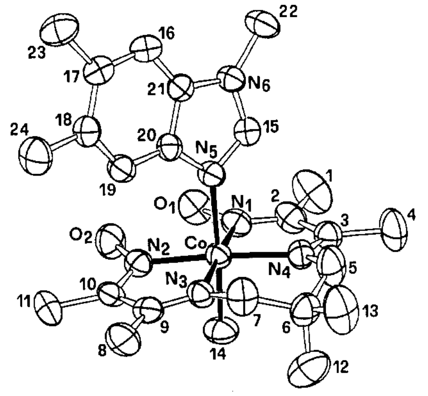

**Figure 2.** ORTEP drawing (50% probability thermal ellipsoids) and labeling scheme for the non-hydrogen atoms of II.

**Solution and Refinement of the Structures.** The structures, solved by conventional Patterson and Fourier methods, were refined by full-matrix anisotropic least-squares refinement. The final cycles included the contribution of H atoms at calculated positions ($B = 1.3B_{eq}$ (Å$^2$)), with the exclusion of those bonded to the disordered atoms in I. The final weighting scheme[18] was $w = 1/(\sigma^2(F) + (0.01F)^2 + q)$, where $q = 1.0$ and 4.0 for I and II, respectively. Atomic scattering factors were those of ref 19. All calculations were carried out by using the SDP-CAD4 programs. Final positional parameters of non-hydrogen atoms and their $B_{eq}$ values (Å$^2$) are given in Table II.

## Results

**Preparations.** Cobalt(III) complexes containing (DH)$_2$ and (DO)(DOH)pn have been synthesized previously by using methods similar to those used here.[1-4,7-15] The relative ease of preparation decreases in the order (DH)$_2$ > (DO)(DOH)pn > (DO)-(DOH)Me$_2$pn.

**Structural Studies.** ORTEP drawings of the cations of I and of II, together with the atom-numbering scheme, are shown in Figures 1 and 2, respectively. In both compounds, the (DO)-(DOH)Me$_2$pn ligand occupies the four equatorial positions of a distorted octahedron. The Co(DO)(DOH)Me$_2$pn units are similar within experimental error. The four equatorial N atoms are coplanar within ±0.022 (4) Å (I) and ±0.008 (4) Å (II), with the cobalt atoms displaced by 0.07 Å (I) and 0.08 Å (II) toward L. The planes of the chemically equivalent halves of the equatorial macrocycle, with the exclusion of propylene bridge atoms, make dihedral angles, $\alpha$, of 10.8° (I) and 13.5° (II) and bend toward the methyl group.

The py and Me$_3$Bzm ligands are planar (within ±0.006 (6) Å (I) and ±0.021 (5) Å (II), respectively), and their mean planes nearly bisect the CH$_3$C–CCH$_3$ bonds of the equatorial moieties.

---

[18] *International Tables for X-ray Crystallography*; Kynoch Press: Birmingham, England, 1974; Vol. IV (present distributor D. Reidel, Dordrecht, The Netherlands).

[19] Zangrando, E.; Bresciani-Pahor, N.; Randaccio, L.; Charland, J.-P.; Marzilli, L. G. *Organometallics* **1986**, *5*, 1938.

**Table II.** Atomic Positional Parameters of Non-Hydrogen Atoms with Esd's in Parentheses

| atom | *x* | *y* | *z* | *B*, Å$^2$ | atom | *x* | *y* | *z* | *B*, Å$^2$ |
|---|---|---|---|---|---|---|---|---|---|
| [py(Co(DO)(DOH)Me$_2$pn)Me]PF$_6$ (I) | | | | | | | | | |
| Co | 0.18812 (5) | 0.02608 (5) | 0.04772 (4) | 2.580 (9) | C11 | 0.5114 (4) | −0.0288 (6) | 0.0533 (4) | 5.5 (1) |
| O1 | 0.2044 (3) | 0.1696 (3) | −0.0909 (2) | 4.16 (8) | C12 | 0.0444 (6) | −0.2122 (6) | 0.1109 (6) | 4.4 (2) |
| O2 | 0.3674 (3) | 0.0865 (3) | −0.0467 (3) | 4.59 (8) | C13 | 0.0042 (5) | −0.1642 (5) | 0.2667 (4) | 5.3 (1) |
| N1 | 0.1408 (3) | 0.1246 (3) | −0.0328 (3) | 2.99 (8) | C14 | 0.2113 (4) | 0.1471 (4) | 0.1285 (4) | 4.0 (1) |
| N2 | 0.3320 (3) | 0.0325 (3) | 0.0206 (3) | 3.31 (8) | C15 | 0.1066 (4) | −0.0875 (4) | −0.1099 (3) | 3.7 (1) |
| N3 | 0.2389 (3) | −0.0637 (3) | 0.1368 (3) | 3.26 (8) | C16 | 0.0995 (5) | −0.1606 (4) | −0.1744 (4) | 4.5 (1) |
| N4 | 0.0423 (3) | 0.0253 (3) | 0.0785 (2) | 2.96 (7) | C17 | 0.1654 (5) | −0.2447 (4) | −0.1732 (4) | 4.9 (1) |
| N5 | 0.1750 (3) | −0.0938 (3) | −0.0445 (3) | 3.37 (7) | C18 | 0.2344 (5) | −0.2534 (5) | −0.1073 (5) | 5.5 (1) |
| C1 | −0.0059 (5) | 0.2329 (4) | −0.0871 (4) | 4.6 (1) | C19 | 0.2378 (4) | −0.1774 (4) | −0.0437 (4) | 5.0 (1) |
| C2 | 0.0420 (4) | 0.1504 (4) | −0.0304 (3) | 3.3 (1) | C6* | 0.061 (2) | −0.075 (2) | 0.216 (1) | 4.4 (4)* |
| C3 | −0.0148 (4) | 0.0921 (4) | 0.0366 (3) | 3.25 (9) | C12* | 0.066 (2) | 0.024 (2) | 0.269 (1) | 5.1 (4)* |
| C4 | −0.1301 (4) | 0.1120 (5) | 0.0509 (4) | 5.0 (1) | P | 0.7128 (1) | 0.0434 (1) | 0.3076 (1) | 5.57 (4) |
| C5 | −0.0012 (4) | −0.0347 (5) | 0.1504 (4) | 5.3 (1) | F1 | 0.6415 (6) | 0.1067 (6) | 0.2443 (4) | 14.7 (2) |
| C6 | 0.0562 (6) | −0.1286 (6) | 0.1828 (5) | 3.8 (1) | F2 | 0.6778 (5) | 0.1182 (5) | 0.3806 (3) | 12.7 (2) |
| C7 | 0.1714 (4) | −0.1114 (4) | 0.2036 (3) | 4.0 (1) | F3 | 0.7792 (5) | −0.0161 (6) | 0.3693 (4) | 18.8 (2) |
| C8 | 0.4005 (5) | −0.1307 (5) | 0.2069 (4) | 4.6 (1) | F4 | 0.7461 (4) | −0.0284 (4) | 0.2276 (3) | 9.9 (1) |
| C9 | 0.3392 (4) | −0.0727 (4) | 0.1399 (3) | 3.35 (9) | F5 | 0.6164 (4) | −0.0248 (5) | 0.3261 (5) | 13.4 (2) |
| C10 | 0.3962 (4) | −0.0198 (4) | 0.0697 (3) | 3.7 (1) | F6 | 0.8056 (5) | 0.1123 (5) | 0.2844 (5) | 15.3 (2) |
| [Me$_3$Bzm(Co(DO)(DOH)Me$_2$pn)Me]PF$_6$ (II) | | | | | | | | | |
| Co | 0.07948 (4) | 0.17107 (4) | 0.07050 (2) | 2.83 (1) | C16 | 0.1394 (4) | 0.4786 (3) | 0.0138 (2) | 3.7 (1) |
| O1 | 0.2780 (2) | 0.1519 (2) | 0.0841 (1) | 4.56 (9) | C17 | 0.1074 (3) | 0.4739 (3) | −0.0392 (2) | 3.5 (1) |
| O2 | 0.2202 (2) | 0.1510 (2) | −0.0101 (1) | 4.60 (9) | C18 | 0.0681 (4) | 0.4042 (3) | −0.0588 (2) | 3.6 (1) |
| N1 | 0.1942 (3) | 0.1587 (2) | 0.1093 (2) | 3.45 (9) | C19 | 0.0630 (4) | 0.3402 (3) | −0.0263 (2) | 3.5 (1) |
| N2 | 0.1275 (3) | 0.1569 (2) | 0.0000 (2) | 3.37 (9) | C20 | 0.0967 (3) | 0.3431 (3) | 0.0273 (2) | 2.94 (9) |
| N3 | −0.0372 (3) | 0.1756 (2) | 0.0315 (2) | 3.31 (8) | C21 | 0.1329 (3) | 0.4130 (3) | 0.0460 (2) | 3.0 (1) |
| N4 | 0.0293 (3) | 0.1757 (2) | 0.1425 (2) | 3.42 (8) | C22 | 0.1951 (4) | 0.4563 (3) | 0.1385 (2) | 4.6 (1) |
| N5 | 0.0993 (3) | 0.2892 (2) | 0.0689 (2) | 3.06 (8) | C23 | 0.1141 (4) | 0.5434 (3) | −0.0759 (3) | 5.0 (1) |
| N6 | 0.1565 (3) | 0.4007 (2) | 0.1001 (2) | 3.38 (9) | C24 | 0.0309 (5) | 0.3990 (4) | −0.1167 (2) | 5.4 (1) |
| C1 | 0.2737 (4) | 0.1456 (4) | 0.1984 (2) | 6.2 (2) | O3 | 0.2035 (7) | 0.3193 (5) | 0.2427 (4) | 7.7 (3) |
| C2 | 0.1885 (4) | 0.1548 (3) | 0.1617 (2) | 4.0 (1) | P | 0.4513 (2) | 0.4198 (1) | 0.24560 (7) | 7.20 (5) |
| C3 | 0.0916 (4) | 0.1659 (3) | 0.1809 (2) | 3.7 (1) | F1 | 0.5528 (7) | 0.4020 (8) | 0.2215 (4) | 16.8 (4) |
| C4 | 0.0702 (5) | 0.1680 (4) | 0.2409 (2) | 6.1 (2) | F2 | 0.5069 (8) | 0.4886 (5) | 0.2709 (4) | 14.1 (3) |
| C5 | −0.0685 (4) | 0.1997 (4) | 0.1546 (2) | 5.4 (1) | F3 | 0.3693 (7) | 0.4579 (7) | 0.2701 (4) | 14.6 (3) |
| C6 | −0.1433 (4) | 0.1760 (4) | 0.1146 (2) | 4.6 (1) | F4 | 0.385 (1) | 0.3562 (8) | 0.2393 (5) | 25.7 (7) |
| C7 | −0.1245 (4) | 0.2045 (4) | 0.0565 (2) | 4.8 (1) | F5 | 0.4901 (9) | 0.3729 (5) | 0.2942 (4) | 15.6 (3) |
| C8 | −0.1112 (4) | 0.1628 (4) | −0.0594 (2) | 5.2 (1) | F6 | 0.4191 (7) | 0.4449 (6) | 0.1907 (3) | 14.3 (3) |
| C9 | −0.0309 (4) | 0.1614 (3) | −0.0197 (2) | 3.6 (1) | F1* | 0.498 (1) | 0.3470 (8) | 0.2292 (8) | 23.5 (6) |
| C10 | 0.0659 (4) | 0.1473 (3) | −0.0386 (2) | 3.5 (1) | F2* | 0.503 (1) | 0.4678 (9) | 0.2084 (6) | 15.4 (5) |
| C11 | 0.0931 (5) | 0.1291 (4) | −0.0962 (2) | 5.5 (1) | F3* | 0.369 (1) | 0.4795 (8) | 0.2340 (8) | 18.3 (6) |
| C12 | −0.1576 (5) | 0.0892 (4) | 0.1146 (3) | 6.7 (2) | F4* | 0.377 (1) | 0.3753 (8) | 0.2831 (6) | 12.7 (4) |
| C13 | −0.2362 (4) | 0.2136 (5) | 0.1328 (3) | 7.4 (2) | F5* | 0.483 (1) | 0.440 (1) | 0.2962 (5) | 21.4 (7) |
| C14 | 0.0756 (4) | 0.0555 (3) | 0.0709 (2) | 4.4 (1) | F6* | 0.412 (1) | 0.3587 (7) | 0.2045 (5) | 13.9 (5) |
| C15 | 0.1350 (3) | 0.3265 (3) | 0.1110 (2) | 3.4 (1) | | | | | |

**Table III.** Selected Bond Lengths (Å) and Bond Angles (deg) for Compounds I and II

| | I | II |
|---|---|---|
| | Bond Lengths | |
| Co–N1 | 1.874 (3) | 1.890 (4) |
| Co–N2 | 1.879 (2) | 1.875 (4) |
| Co–N3 | 1.908 (3) | 1.906 (4) |
| Co–N4 | 1.914 (2) | 1.907 (4) |
| Co–N5 | 2.105 (3) | 2.076 (3) |
| Co–C14 | 2.017 (3) | 2.015 (4) |
| | Bond Angles | |
| N1–Co–N2 | 97.8 (1) | 98.1 (2) |
| N1–Co–N3 | 174.7 (1) | 175.8 (2) |
| N1–Co–N4 | 81.8 (1) | 81.7 (2) |
| N1–Co–N5 | 91.2 (2) | 90.5 (2) |
| N1–Co–C14 | 86.3 (1) | 84.6 (2) |
| N2–Co–N5 | 87.6 (1) | 93.7 (2) |
| N2–Co–C14 | 87.8 (1) | 83.3 (2) |
| N3–Co–N5 | 94.0 (1) | 93.8 (2) |
| N3–Co–C14 | 88.5 (1) | 91.2 (2) |
| N4–Co–N5 | 95.1 (2) | 91.4 (2) |
| N4–Co–C14 | 89.5 (1) | 91.6 (3) |
| Co–N5–C15 | 121.2 (2) | 121.7 (3) |
| Co–N5–C19 | 122.4 (3) | |
| C15–N5–C19 | 116.4 (4) | |
| Co–N5–C20 | | 132.9 (4) |
| C15–N5–C20 | | 104.6 (4) |

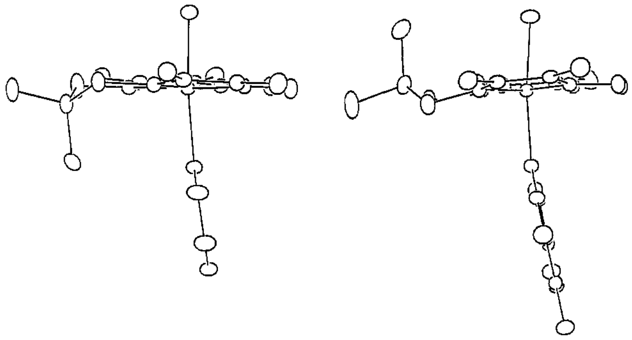

Figure 3. Side view of the cation I (left, disordered atoms at low occupancy not reported) and II (right).

The absolute values of the torsion angle $\phi$, (C15–N5–Co–N*; N* is the midpoint between N1 and N2) are 75.8° (I) and 87.1° (II). The neutral ligand planes make angles $\gamma$ of 82.3° (I) and 81.0° (II) with the least-squares plane of the four equatorial N atoms. These angles are an estimate of the tilt of L with respect to the axial direction (Figure 3).

The L–Co–$CH_3$ fragment is characterized by a N–Co–C angle of 174.5 (1)° (I) and of 173.8 (2)° (II). The Co–N axial distances are 2.105 (3) and 2.076 (3) Å, respectively, whereas the Co–C bond lengths of 2.017 (3) Å in I and 2.014 (5) Å in II are similar within the experimental error. The other bond lengths and angles are in the range usually observed for complexes containing the (DO)(DOH)pn ligand.[9,13]

A disordered propylene bridge was interpreted as due to two orientations, nearly related by a mirror plane passing through the

**Table IV.** First-Order Rate Constants ($s^{-1}$) for L Exchange of $LCo(CHEL)CH_3$ in $CH_2Cl_2$ at 25 °C

| L | $[LCo((DO)(DOH)Me_2pn)CH_3]^{+a}$ | $[LCo((DO)(DOH)pn)CH_3]^{+c}$ | $LCo(DH)_2CH_3{}^d$ |
|---|---|---|---|
| $PhNH_2$ | $7.90 \pm 0.5^b$ | $(5.0 \pm 0.1) \times 10^{-1}$ | $1.50 \pm 0.04$ |
| $MeOPhNH_2$ | $3.32 \pm 0.2$ | $(9.0 \pm 0.2) \times 10^{-2}$ | $(4.70 \pm 0.1) \times 10^{-1\,e}$ |
| 1,2-$Me_2$Imd | $(4.20 \pm 0.3) \times 10^{-1}$ | $(5.9 \pm 0.3) \times 10^{-2}$ | $(1.1 \pm 0.1) \times 10^{-2}$ |
| $Me_3$Bzm | $(6.21 \pm 0.3) \times 10^{-1}$ | $(4.34 \pm 0.06) \times 10^{-2}$ | $(4.19 \pm 0.04) \times 10^{-3\,f}$ |
| py | $1.32 \pm 0.06$ | $(3.4 \pm 0.1) \times 10^{-2}$ | $(8.0 \pm 0.8) \times 10^{-3}$ |
| 3,5-LUT | $(9.54 \pm 0.22) \times 10^{-1}$ | $(1.5 \pm 0.1) \times 10^{-2}$ | $(2.36 \pm 0.06) \times 10^{-3\,c}$ |
| DEA | $(5.26 \pm 0.13) \times 10^{-2}$ | $(7.7 \pm 0.1) \times 10^{-4}$ | $(5.4 \pm 0.2) \times 10^{-3\,e}$ |
| 4-$Me_2$Npy | $(1.23 \pm 0.01) \times 10^{-2}$ | $(5.6 \pm 0.1) \times 10^{-4}$ | $(1.89 \pm 0.05) \times 10^{-4\,c}$ |
| 1-MeImd | $(5.71 \pm 0.1) \times 10^{-3}$ | $(9.9 \pm 0.1) \times 10^{-5}$ | $(1.78 \pm 0.02) \times 10^{-4\,c}$ |
| $P(OMe)_3$ | $(3.45 \pm 0.06) \times 10^{-2}$ | $(7.17 \pm 0.08) \times 10^{-4\,d}$ | $(4.1 \pm 0.2) \times 10^{-3}$ |
| $PEtPh_2$ | $(1.58 \pm 0.03) \times 10^{-2}$ | $(1.90 \pm 0.02) \times 10^{-4\,d}$ | $(1.1 \pm 0.1) \times 10^{-4}$ |
| $POEtPh_2$ | $(2.32 \pm 0.2) \times 10^{-3}$ | $(8.27 \pm 0.01) \times 10^{-5\,d}$ | $(7.7 \pm 0.5) \times 10^{-4\,e}$ |

[a] This work ($PF_6^-$ salt). [b] Average of two rate measurements. [c] References 9 and 13 unless specified otherwise ($ClO_4^-$ salt). [d] Reference 3 unless specified otherwise. [e] Reference 7 and: Bayo, F. Unpublished studies. [f] Reference 6.

**Table V.** $^1H$ Chemical Shifts (ppm) of Imidazole Ligands and Their $(DH)_2$, (DO)(DOH)pn,[a] and $(DO)(DOH)Me_2pn$ Compounds[a]

| | $N-CH_3$ | $H2/CH_3$ | H4 | H5/H7 |
|---|---|---|---|---|
| 1-MeImd | 3.68 | 7.41 | 7.03 | 6.87 |
| $(DH)_2{}^b$ | 3.64 | 7.44 | 6.96 | 6.78 |
| (DO)(DOH)pn | 3.71 | 7.24 | 6.41 | 6.84 |
| $(DO)(DOH)Me_2pn$ | 3.72 | 7.12 | 6.20 | 6.85 |
| 1,2-$Me_2$Imd | 3.52 | 2.37 | 6.87 | 6.77 |
| $(DH)_2{}^b$ | 3.48 | 2.32 | 7.12 | 6.66 |
| (DO)(DOH)pn | 3.52 | 2.06 | 6.16 | 6.80 |
| $(DO)(DOH)Me_2pn$ | 3.52 | 1.88 | 5.84 | 6.70 |
| $Me_3$Bzm | 3.75 | 7.71 | 7.47 | 7.17 |
| $(DH)_2{}^b$ | 3.75 | 7.90 | 7.93 | 7.13 |
| (DO)(DOH)pn[c,d] | 3.81 | 7.29 | 7.07 | 7.20 |
| $(DO)(DOH)Me_2pn$[d] | 3.81 | 7.04 | 6.65 | 7.22 |

[a] $PF_6^-$ salts. [b] References 6, 9, and 13. [c] Reference 9. [d] $CD_2Cl_2$.

**Chart I**[a]

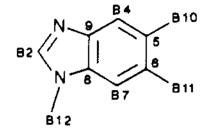

[a] The "B" designation for the carbon atoms refers to the benzimidazole ring.

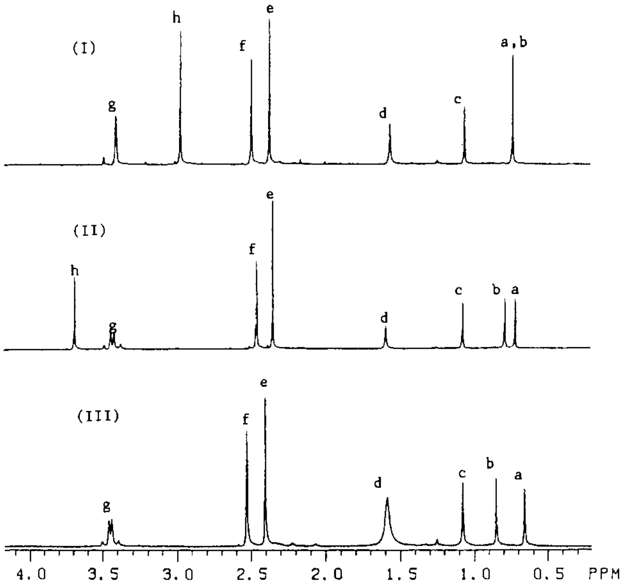

**Figure 4.** Partial $^1H$ NMR spectra of $[LCo((DO)(DOH)Me_2pn)CH_3]PF_6$ in $CDCl_3$: (I) L = 4-$Me_2$Npy; (II) L = 1-MeImd; (III) L = py. Signals: (a–c) Co—$CH_3$ and methyls on the propylene bridge; (d) $H_2O$; (e) O—N=$CCH_3$; (f) C—N=$CCH_3$; (g) $NC^*H_2C(CH_3)_2C^*H_2N$; (h) N—$CH_3$.

N3, N4, C5, C7, and C13 atoms, with occupancy factors of 0.7 and 0.3, respectively (Figure 1). Two orientations of the $PF_6^-$ anion (0.6 and 0.4 occupancies) and a crystallographically independent water of crystallization with half-occupancy were found in II. The starred symbols indicate the atoms of lowest occupancies. The O···O distances of the oxime bridges are 2.430 (5) Å (2) and 2.453 (5) Å (II).

**Rate Measurements.** Ligand exchange rates for all 12 $[LCo((DO)(DOH)Me_2pn)CH_3]PF_6$ complexes in $CH_2Cl_2$ were first-order in [Co]. Variation of the concentration of entering ligand (L′) from 10 to 100 times that of [Co] did not significantly change $k_{obs}$. Therefore, the rate expression is consistent with an $S_N1$ LIM reaction and $k_{obs} = k_1$ (Table IV).

**$^1$H NMR.** The $^1H$ NMR chemical shift data of all new organocobalt complexes are given in Tables V, SII, and SIII (Table SII and SIII are given as supplementary material). 2D- and 1D-NOE experiments were performed on the 1-MeImd and $Me_3$Bzm complexes.

For the 1-MeImd complex, all the expected 2D-NOE crosspeaks were not observed and 1D-NOE experiments were needed. In the 1D-NOE experiment, saturation of the N–$CH_3$ signal gave crosspeaks to the neighboring protons (H2 and H5). The unaffected signal is assigned to H4. Partial saturation of the H4 signal allowed assignment of the H5 and, hence, H2 signals. In the 2D-NOE experiment, used to assign the remaining signals of the 1-MeImd complex, the O-H-O signal at 18.58 ppm has a crosspeak to the methyl signal at 2.36 ppm (O—N=C—$CH_3$). The methylene signals of the equatorial ligand at 3.46 ppm have crosspeaks with the two methyl signals at 0.73 and 1.07 ppm, indicating that these are for the methyls of the propylene bridge and that the methyl peak at 0.85 ppm is for Co–$CH_3$. In addition, an NOE crosspeak from the Co–$CH_3$ signal to that at 1.07 ppm assigns this signal to the propylene $CH_3$ closest to Co–$CH_3$.

Similarly, the H2, H4, H7 and $(B12)H_3$ signals (see Chart I) of the $Me_3$Bzm complex have been assigned from the 2D-NOE experiment (Table V). The two signals at 2.28 and 2.36 ppm are assigned to $(B10)H_3$ and $(B11)H_3$, respectively. The two methyl signals at 0.83 and 0.87 ppm are not resolved well, but one signal must be for Co–$CH_3$ and the other for one of the bridge $CH_3$ groups (Table SII).

The assignment of protons of other complexes was made by analogy with the chemical shifts of the well-characterized (DO)(DOH)pn analogues.[9]

The methylene protons of the equatorial ligand (2.7–3.6 ppm) in this study are not equivalent and give an AB coupling pattern (Figure 4). In the 4-$Me_2$Npy complex, however, a singlet is observed. The $^1H$ NMR spectra (upfield region) of the complexes with L = 1-MeImd, 4-$Me_2$Npy, and py(I) are shown in Figure 4.

Of greatest interest, the change of the equatorial ligand from (DO)(DOH)pn to $(DO)(DOH)Me_2pn$ leads to upfield shifts of the signals of the L protons close to the coordination center. In the imidazole-type ligands, the signals that are shifted more upfield are those for H2 and H4 (Table V). This effect is more pronounced in the complex of the bulky $Me_3$Bzm ligand. For ex-

**Table VI.** Chemical Shifts of $^{13}C$ NMR Signals for $Me_3Bzm$ and for $Me_3BzmCo(CHEL)CH_3$ Complexes in DMSO-$d_6$[a]

| compd | B2 | B4 | B5 | B6 | B7 | B8 | B9 | B10 | B11 | B12 |
|---|---|---|---|---|---|---|---|---|---|---|
| $Me_3Bzm$ | 143.56 | 119.30 | 130.77 | 129.60 | 110.05 | 133.13 | 142.00 | 20.03 | 19.83 | 30.49 |
| $Me_3Bzm + H^+$ | 140.39 | 114.04 | 135.49 | 135.87 | 112.57 | 130.16 | 128.89 | 19.90 | 19.74 | 32.82 |
| CHEL | B2 | B4 | B5 | B6 | B7 | B8 | B9 | B10 | B11 | B12 |
| $(DO)(DOH)Me_2pn$[b] | 143.78 | 116.08 | 132.49 | 131.76 | 111.50 | 133.41 | 139.43 | 20.32 | 19.80 | 31.51 |
| (DO)(DOH)pn[b] | 144.29 | 116.45 | 132.55 | 131.74 | 111.34 | 133.18 | 139.41 | 20.34 | 19.71 | 31.53 |
| $(DH)_2$ | 143.75 | 117.88 | 132.14 | 131.17 | 110.69 | 132.75 | 139.73 | 20.12 | 19.79 | 31.34 |

[a] The values for the chemical shifts (ppm) for $(DO)(DOH)Me_2pn$ and (DO)(DOH)pn respectively are as follows: $C{=}N{-}CH_3$, 174.98, 173.13; $O{-}N{=}CH_3$, 154.20, 153.90; $NC^*H_2CR_2C^*H_2N$, 59.43, 48.79; $NCH_2C^*R_2CH_2N$, 36.80, 26.98; $C{-}N{=}C^*CH_3$, 17.49, 17.12; $O{-}N{=}C{-}C^*H_3$, 12.61, 12.61; $NCH_2C(C^*H_3)_2CH_2N$, 26.03 and 24.96. R = H for (DO)(DOH)pn; R = $CH_3$ for $(DO)(DOH)Me_2Pn$. [b] $PF_6^-$ salts; (DO)(DOH)pn from ref 9.

**Table VII.** Comparison of Geometrical Parameters of $LCo(CHEL)CH_3$ with CHEL = $(DO)(DOH)Me_2pn$, (DO)(DOH)pn, and $(DH)_2$ and L = py and $Me_3Bzm$

| | $(DO)(DOH)Me_2pn$[a] | | (DO)(DOH)pn | | $(DH)_2$ | |
|---|---|---|---|---|---|---|
| | py | $Me_3Bzm$ | py[b] | $Me_3Bzm$[c] | py[d] | $Me_3Bzm$[e] |
| Co–N, Å | 2.105 (3) | 2.076 (3) | 2.106 (3) | 2.100 (3) | 2.068 (3) | 2.060 (2) |
| Co–C, Å | 2.017 (3) | 2.014 (5) | 2.003 (3) | 2.011 (3) | 1.998 (5) | 1.989 (2) |
| $\alpha$, deg[f] | +10.4 | +16.5 | +6.9 | +13.8 | +3.2 | +4.7 |
| $d$, Å[f] | +0.07 | +0.08 | +0.07 | +0.09 | +0.04 | +0.06 |
| $\phi$, deg[g] | 75.8 | 87.1 | 96.4 | 115.1 | ~0 | ~0 |
| $\gamma$, deg[g] | 82.3 | 81.0 | 89.6 | 87.3 | ~90 | ~90 |
| C6↑[h] | py | $CH_3$ | $CH_3$ | $Me_3Bzm$ | | |

[a] Present work. [b] Reference 13. [c] Reference 9. [d] Reference 3. [e] Reference 6. [f] Positive values of $\alpha$ and $d$ indicate a bending of the equatorial ligand toward the methyl group and displacement of Co out of the four N equatorial donor set toward L. [g] For definition of $\phi$ and $\gamma$, see text. [h] C6↑ indicates on which side of the axial ligands, L or $CH_3$, the C6 atom lies.

ample, the H4 signal of $Me_3Bzm$ in the spectrum of the $(DO)(DOH)Me_2pn$ derivative is 0.42 ppm further upfield than that of its (DO)(DOH)pn analogue, whereas the H4 signal of 1-MeImd is shifted upfield by only 0.21 ppm for a similar comparison. Likewise, the $\alpha$-H signals of L in the pyridine-type complexes of $(DO)(DOH)Me_2pn$ are upfield to those of the (DO)(DOH)pn analogues.

**$^{13}C$ NMR.** The $^{13}C$ assignments of $Me_3Bzm$ in the $(DO)(DOH)Me_2pn$ complex are based on those of the (DO)(DOH)pn analogue[9] and free $Me_3Bzm$[6] (Table VI). The $^{13}C$ signals of B2 and B4 in $(DO)(DOH)Me_2pn$ are shifted upfield by 0.51 ppm and 0.37 ppm, respectively, as compared to those in the (DO)(DOH)pn analogue,[9] whereas the remaining shifts are very similar to those of the analogue.

## Discussion

**Structural Comparisons.** In Table VII some geometrical features of I and II are compared with those of the corresponding (DO)(DOH)pn and $(DH)_2$ derivatives. Although the Co–$CH_3$ bond lengths are practically independent of CHEL, the Co–N(axial) distances for cobaloximes are significantly shorter, a difference previously attributed to the different orientation of the planar L ligand.[9] In the cobaloximes the $\phi$ angle is close to 0°, while in the other complexes it varies from 76 to 115°. The Co–$Me_3Bzm$ axial bond length in II is shorter and C6 has the opposite relation with respect to the equatorial ligand compared to that in the (DO)(DOH)pn analogue. These differences are small and may be due to packing forces. The most unusual feature of the structural comparisons in Table VII is the low values of $\gamma$ for I and II, with the L ligands tilted away from the $Me_2pn$ bridge, suggesting steric interactions.

**Reaction Rates.** The rates of ligand dissociation are approximately 10–$10^2$ times greater for $[LCo((DO)(DOH)Me_2pn)R]X$ complexes than for the analogous $[LCo((DO)(DOH)pn)R]X$ complexes despite the evidence (vide infra) that the electronic properties of the Co center are also similar. Therefore, the difference in rates most probably is steric in origin, as suggested by the X-ray structures.

**$^1H$ NMR.** The steric effect of the methyl substituents on the propylene bridge is clearly evident in several features of the $^1H$ NMR spectrum. As stated above, one of our major goals in carrying out this study was to gain a greater understanding of factors influencing NMR chemical shifts in organocobalt compounds. Previous studies have identified Co anisotropy, equatorial ligand anisotropy, and electronic through-bond effects as contributing to chemical shifts.[3,6,9]

On the basis of the downfield shifts of L signals remote from the Co center for Costa-type complexes being greater for cobaloximes, we concluded that the Co center was more electrophilic in the Costa-type compounds than in cobaloximes.[9,13] On the other hand, signals for ligand nuclei close to the Co(CHEL) moiety are further upfield for Costa-type compounds than for cobaloximes, suggesting the former have greater anisotropy in the Co(CHEL) moiety.

This anisotropy could arise from the Co center itself or from the CHEL double bonds. Obviously, the increased bulk of the propylene chain in Costa compounds in comparison to the N–O–H···O–N group in cobaloximes favors orientations of L with $\phi \approx 90°$, where L atoms closest to the equatorial ligand lie close to the double bonds. On the other hand, double bonds in the Costa-type complexes are different from those in dioximato ligands of cobaloximes. Therefore, the origin of the greater anisotropy of Co(CHEL) in Costa-type compounds is unclear.

This situation is greatly simplified when the electronically very similar CHEL ligands (DO)(DOH)pn and $(DO)(DOH)Me_2pn$ are compared. The $Me_2pn$ group should force planar L ligands to lie over the double bonds. When $^1H$ NMR signals remote from the Co are compared for the two systems, the shifts are very similar (Tables V and SIII). However, when $^1H$ signals of L nuclei close to the Co(CHEL) region are compared, the signals are to higher field for the $Co(DO)(DOH)Me_2pn$ system. This result strongly suggests that a major component of the Co(CHEL) anisotropy in the Costa-type system is due to anisotropy of the CHEL ligand. Consistent with this conclusion, the NH signals of amine ligands (Table SIII) which can not be influenced by CHEL anisotropy are further downfield in the Costa systems compared to the signals for cobaloximes.

**$^{13}C$ NMR.** The $^{13}C$ NMR results, although limited, support our conclusions concerning the origins of anisotropy. The $^{13}C$ shifts for atoms remote from the Co(CHEL) moiety have similar shifts for the two Costa-type complexes, whereas $^{13}C$ shifts for atoms close to Co(CHEL) (B2, B4) are relatively upfield for the $(DO)(DOH)Me_2$ pn complexes.

Recently, the factors influencing $^{13}C$ NMR shifts of organocobalt compounds have been the subject of intense study.[5-9] Part of the reason for this interest is that modern NMR methods allow assignment of the signal in compounds as complex as cobalamins.[5] The relationship between the assigned shifts and structure could be helpful in studies of $B_{12}$ holoenzymes.

Several approaches have been employed to interpret $^{13}C$ shifts either as a function of structure[3] or as a function of the electronic influence of the R axial substituent.[7,19] These effects are closely, although probably not directly, related since good electron donor R groups lead to upfield $^{13}C$ NMR shifts of axial L that closely parallel increases in Co–L bond lengths.

Since $H^+$ is a pure electrophile, Brown suggested[8] that the effects of the $H^+$ give some indication of the consequences of electron withdrawal, particularly for C atoms remote from BN3. We compare (Table VI) the effect of $Co(CHEL)CH_3$ and $H^+$ on the $^{13}C$ shifts of $Me_3Bzm$. It is noteworthy that B9 is most affected by $H^+$, shifting upfield by ca. 13 ppm. All the $Co(CHEL)CH_3$ moieties shift this signal upfield; the Costa complexes have roughly similar effects, which are slightly greater than that of the $Co(DH)_2CH_3$ moiety. The same relationship holds for B5, B6, B7, and B12 shifts, which are futher downfield for Costa-type compounds than cobaloximes, consistent with the lower electrophilicity of Co in the latter. However, the B8 shift (which should be minimally affected by anisotropy) is anomalous in the Costa-type system, shifting downfield rather than upfield, as expected. For B2, all three $Co(CHEL)CH_3$ electrophiles shift the $^{13}C$ signal in the direction opposite to that expected from protonation.

Our findings demonstrate that expressions to account for changes in chemical shifts as a function of R in organocobalt complexes must incorporate CHEL anisotropy. A rigid system may be required to assess all contributions fully since the anisotropic contribution of the CHEL portion of Co(CHEL) is not uniform in the equatorial plane and since rotation of L around the Co–L bond will lead to a family of conformations. The population distribution of these conformers may depend on the bulk of R as well as the solvent, the electronic effect of R (i.e., the length of the Co–L bond), etc. Ironically, since the position of the 5,6-dimethylbenzimidazole moiety in cobalamins is relatively fixed, the CHEL ligand contribution may be easier to assess than in model compounds. However, the sparsity and low accuracy of cobalamin X-ray structures make overall interpretation of shifts more complex for cobalamins. Clearly, NMR spectroscopy has given us greater insight into the properties of both models and cobalamins but a deeper understanding is needed before the conformation of $B_{12}$ in holoenzymes can be interpreted by NMR methods.

**Acknowledgment.** This research was supported by NIH Grant GM 29225 to L.G.M. and by a grant from the MPI (Rome) to L.R. The purchase of the NMR instruments was supported in part by NSF departmental grants to Emory University. We are grateful to these organizations.

**Supplementary Material Available:** Tables of analytical data, additional NMR data, complete bond lengths and bond angles, hydrogen atom positional parameters, and general displacement expressions for compounds I and II, figures of the absolute-value-mode 2N NOE spectra of $[Me_3BzmCo((DO)(DOH)Me_2pn)CH_3]PF_6$ and of $[1\text{-MeImdCo}((DO)(DOH)Me_2pn)CH_3]PF_6$, and an identifying figure for $^1H$ NMR chemical shifts (ppm) of $[1\text{-MeImdCo}((DO)(DOH)Me_2pn)]PF_6$ in $CDCl_3$ (16 pages); tables of observed and calculated structure factors for compounds I and II (14 pages). Ordering information is given on any current masthead page.

---

Contribution from the Department of Applied Chemistry, Faculty of Engineering,
Osaka University, Yamadaoka, Suita, Osaka 565, Japan

# Spectroscopic and Electrical Properties of $VO(dmit)_2$ and $V(dmit)_3$ Anion Complexes and X-ray Crystal Structure of $[NMP]_2[V(dmit)_3]$ (dmit = 2-Thioxo-1,3-dithiole-4,5-dithiolate, NMP = *N*-Methylphenazinium)

Gen-etsu Matsubayashi,* Kazuki Akiba, and Toshio Tanaka

*Received May 3, 1988*

$V^{IV}O(dmit)_2$ and $V^{IV}(dmit)_3$ anion complexes were prepared. Although they are essentially insulators, their oxidized complexes $[N\text{-methylphenazinium}]_2[V(dmit)_3]$, $[\text{tetrathiafulvalenium}]_2[V(dmit)_3]$, and $[NBu^n{}_4]_{0.17}[V(dmit)_3]$ as well as $[N\text{-methylpyridinium}]_2[VO(dmit)_2]\cdot I_{4.2}$ and $[NBu^n{}_4]_2[V(dmit)_3]\cdot I_{5.4}$ exhibit semiconductive behavior with electrical conductivities of $1 \times 10^{-8}$–$1 \times 10^{-2}$ S $cm^{-1}$. Electronic, ESR, and X-ray photoelectron spectra of these complexes are discussed on the basis of interactions between the anion moieties. A single-crystal X-ray structure analysis of $[N\text{-methylphenazinium}]_2[V(dmit)_3]$, $[C_{13}H_{11}N_2]_2[V(C_3S_5)_3]$, revealed a distorted-octahedral geometry of the $V(dmit)_3$ anion and a layer packing of the anions in the crystal phase. The orthorhombic crystal, space group *Pbca*, has cell dimensions $a = 18.5299$ (6) Å, $b = 30.726$ (2) Å, $c = 14.826$ (1) Å, $V = 8441$ (1) Å$^3$, and $Z = 8$. Block-diagonal least-squares refinement based on 5601 independent reflections with $|F_o| > 3\sigma(F)$ yielded an $R$ factor of 0.056.

## Introduction

In the design of electrically conducting organic compounds, two- or three-dimensional molecular interactions have been focused upon since organic superconductors such as tetramethyltetraselenasulvalene (TMTSF)[1] and bis(ethylenedithio)tetrathiafulvalene (BEDT-TTF) salts[2] were reported. Metal complexes with the 2-thioxo-1,3-dithiole-4,5-dithiolate ligand ($dmit^{2-}$, A) form two- or three-dimensional conduction pathways through contacts between the ligand sulfur atoms in the crystal phase. Several $(dmit)_2$metalate anion complexes (M = Ni, Pd, Pt) with high electrical conductivities have been reported,[3] of which $[TTF][Ni(dmit)_2]_2$ (TTF = tetrathiafulvalene) becomes a superconductor, although only under pressure and at low temperature.[3b,4]

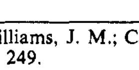

A

---

(1) For a review, see: Williams, J. M.; Carneiro, K. *Adv. Inorg. Chem. Radiochem.* **1985**, *29*, 249.

(2) (a) Urayama, H.; Yamochi, H.; Saito, G.; Nozawa, K.; Sugano, T.; Kinoshita, M.; Sato, S.; Oshima, K.; Kawamoto, A.; Tanaka, J. *Chem. Lett.* **1988**, 55 and references therein. (b) Urayama, H.; Yamochi, H.; Saito, G.; Sato, S.; Kawamoto, A.; Tanaka, J.; Mori, T.; Maruyama, Y.; Inokuchi, H. *Chem. Lett.* **1988**, 463.

(3) (a) Papavassiliou, G. C. *Z. Naturforsch., B* **1982**, *37*, 825. Valade, L.; Bousseau, M.; Gleizes, A.; Cassoux, P. *J. Chem. Soc., Chem. Commun.* **1983**, 110. Valade, L.; Cassoux, P.; Gleizes, A.; Interrante, L. *J. Phys., Colloq.* **1983**, *C3*, 1183. Valade, L.; Legos, J.-P.; Bousseau, M.; Cassoux, P.; Garbauskas, M.; Interrante, L. V. *J. Chem. Soc., Dalton Trans.* **1985**, 783. Bousseau, M.; Valade, L.; Bruniquel, M.-F.; Cassoux, P.; Garbauskas, M.; Interrante, L.; Kasper, J. *Nouv. J. Chim.* **1984**, *8*, 3. Kato, R.; Mori, T.; Kobayashi, A.; Sasaki, Y.; Kobayashi, H. *Chem. Lett.* **1984**, 1. Kato, R.; Kobayashi, H.; Kobayashi, A.; Sasaki, Y. *Chem. Lett.* **1984**, 191. Kim, H.; Kobayashi, A.; Sasaki, Y.; Kato, R.; Kobayashi, H. *Chem. Lett.* **1987**, 1799. (b) Bousseau, M.; Valade, L.; Legros, J.; Cassoux, P.; Garbauskas, M.; Interrante, L. V. *J. Am. Chem. Soc.* **1986**, *108*, 1908. Brossard, L.; Ribault, M.; Bousseau, M.; Valade, L.; Cassoux, P. *C. R. Acad. Sci., Ser. 2* **1986**, *302*, 205.